Int. J. Electrochem. Sci., 14 **(2019)** 2136 – 2159, doi: 10.20964/2019.03.06

International Journal of ELECTROCHEMICAL SCIENCE
www.electrochemsci.org

Effects of Voltage Gradients on Electro-Osmotic Characteristics of Taizhou Soft Clay

Shen Yang[1,2,*], *Feng Jianting*[1,2], *Shi Wen*[1,2], *Qiu Chenchen*[1,2]

[1] Key Laboratory of Geomechanics and Embankment Engineering of Ministry of Education, Hohai University, Nanjing, 210098, P. R. China.
[2] Jiangsu Research Center for Geotechnical Engineering Technology, Hohai University, Nanjing, 210098, P. R. China.
[*]E-mail: shenyang1998@163.com

Received: 1 November 2018 / *Accepted:* 7 January 2019 / *Published:* 7 February 2019

To study the electro-osmotic characteristics of Taizhou soft clay under different voltage gradients, a series of laboratory electro-osmotic experiments with different voltage gradients were conducted. The electro-osmotic treatment effects of these tests were compared by monitoring the drainage, current, voltage, soil element mass fraction and soil structure. The electro-osmotic method was further studied from a theoretical perspective based on the inherent link between macro-level and micro-level indexes. The results showed that the drainage was effectively improved with an increasing voltage gradient when the voltage gradient was within the range of 1 V/cm~2 V/cm, but no significant improvement was observed when the voltage gradient was further increased. Although an excessively high voltage gradient increased the drainage, it also led to greater energy consumption per unit volume of drainage. An increased voltage gradient improved only the proportion of the effective voltage in the early stage of the electro-osmotic process; from a long-term perspective, an excessively high voltage gradient was not useful for increasing the ratio of the effective voltage to the output voltage. Na^+ was the main active ion in Taizhou soft clay during the electro-osmotic process and was the key factor that affected the drainage and drainage velocity. When the voltage gradient was within the range of 1 V/cm~2 V/cm, the concentration of migratory Na^+ increased with an increasing voltage gradient, but no significant improvement was detected when the gradient was further increased. The structure of Taizhou soft clay changed from flocculent to granular after electro-osmotic treatment when the voltage gradient was within the range of 1 V/cm~1.5 V/cm and from flocculent to schistose after electro-osmotic treatment when the voltage gradient was within the range of 1.75 V/cm~2.25 V/cm. Finally, based on the inherent link between the macro and micro levels, a new one-dimensional electro-osmotic consolidation equation that can accurately forecast changes in the excess pore water pressure during electro-osmotic treatment was deduced considering variations in the effective voltage.

Keywords: Voltage gradients; Electrochemical problem; Microscopic active ion; Soil structure; New one-dimensional electro-osmotic consolidation equation.

1. INTRODUCTION

Marine soft clay sediments are extensively distributed along the shoreline in Taizhou, China. This clay has unique properties, such as a high water content, high compressibility, low penetrability, low shear strength and high liquid limit [1]. These properties are highly inconvenient to construction projects. Accordingly, to satisfy the needs of practical applications, foundations composed of soft clay must be processed before construction can begin. The effects of the particle size and porosity of soft clay on the electro-osmotic drainage velocity are negligible [2]. Thus, compared with traditional precompression and dynamic compaction techniques, electro-osmotic methods provide significant advantages for treating low-permeability soft clays [3]. In recent years, many scholars have studied a variety of electro-osmotic methods and techniques, such as electrode conversion and current intermittence in addition to other technologies for improving anode contact by injecting chemical solutions, to improve the effects of electro-osmotic treatment [4-6]. A new class of materials named electrokinetic geosynthetics (EKG) has been used as test electrodes to control electrochemical reactions [7-9], and various forms of electrodes and electrode arrays have been studied to investigate their effects on the electro-osmotic drainage velocity [10-11]. Theoretical studies have been performed on electro-osmosis from an electrochemistry perspective [12]. In addition, the combinations of electro-osmosis with other loading methods, such as the vacuum preloading and heaped load methods, have also been investigated [13-14]. However, while, these studies have contributed immeasurably to the development and application of electro-osmosis, electro-osmotic methods have not become widely available for practical engineering, mainly because the electrochemical problems involved in the electro-osmotic process are extremely complicated. These complexities lead to substantial variations in the electro-osmotic effect due to differences in the physical and chemical properties of soil samples [15]. Therefore, certain fundamental problems, such as the effects of different voltage gradients on electro-osmotic characteristics, must be studied before the electro-osmotic method can be implemented.

According to the work of Wu, Li and Asavadorndeja, the voltage gradients used in laboratory tests are usually within the range of 1 V/cm~2 V/cm [16-18]. On the one hand, an electro-osmotic flow cannot be driven effectively if the voltage gradient is excessively low. On the other hand, an excessively high voltage gradient will create significant exothermic effects and lead to an increase in energy consumption during the electro-osmotic process; moreover, the water content of the anode will decrease quickly, which will affect the conductivity, thereby resulting in failure of the electro-osmotic process.

Taizhou soft clay was taken as the research object in this work to thoroughly explore the electro-osmotic characteristics of such soft clay under different voltage gradients. Electro-osmotic indoor experiments were conducted under five voltage gradients of 1 V/cm, 1.5 V/cm, 1.75 V/cm, 2 V/cm and 2.25 V/cm. The results were analyzed in detail from macro, micro and theoretical perspectives. The variations in the macroscopic properties of the clay were explored, and reasonable explanations were provided based on micro-level considerations. Finally, the electro-osmotic method was theoretically investigated according to the inherent link between the macro and micro levels, following which a new one-dimensional electro-osmotic consolidation equation was deduced. The electro-osmotic characteristics were further discussed to provide references for the application of electro-osmotic methods in the treatment of soft clay foundations.

2. MATERIALS AND METHODS

2.1 Experimental apparatus

The horizontal electro-osmotic test model is composed simply of a sample slot and a collection tank (see Fig. 1). The internal dimensions of the model are 250 mm × 200 mm × 200 mm (L × H × W).

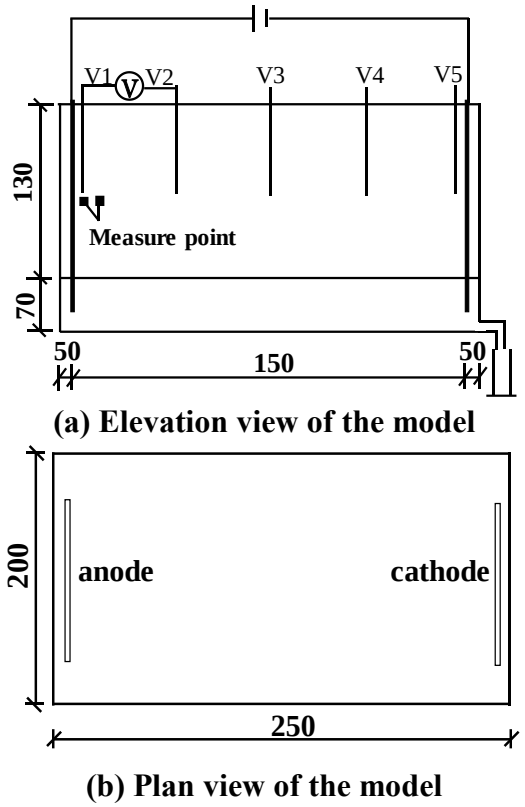

Figure 1. Diagram of the electro-osmotic model (units: mm)

The sample slot, which is 130 mm high, is used for loading soil samples, while the collection tank, which is 70 mm high, has a hole at the bottom for collecting water discharged during the electro-osmotic process. Other major experimental components include a regulated DC power supply (IT6863A) and a multimeter. The soil samples used in the tests were taken from a construction site employing vacuum preloading in Taizhou. The physical and mechanical properties of the soil samples are summarized in Table 1.

Table 1. Physical and mechanical properties of the soil samples

Specific gravity	Liquid limit	Plastic limit	Plasticity index	Soil particle composition		
				Sand	Silt	Clay
2.62	39%	21%	18%	0%	79%	21%

Furthermore, EKG materials, which can not only provide filter and drainage channels but also

accelerate the soil consolidation and the dissipation of excess pore water pressure, can be used as both cathodes and anodes [19]. Based on the abovementioned advantages, a tabular EKG was used as the test electrode. A photograph of the material is shown in Fig. 2, and the corresponding schematic diagram is presented in Fig. 3. The shape of the tabular EKG is similar to that of a plastic drainage board, which is used in vacuum preloading. The EKG is composed of a substrate and a geomembrane in addition to numerous wires. The substrate is made of conductive plastics, and both sides of the substrate are covered with grooves to facilitate drainage. Two copper wires that can be connected to the power supply are embedded inside the substrate.

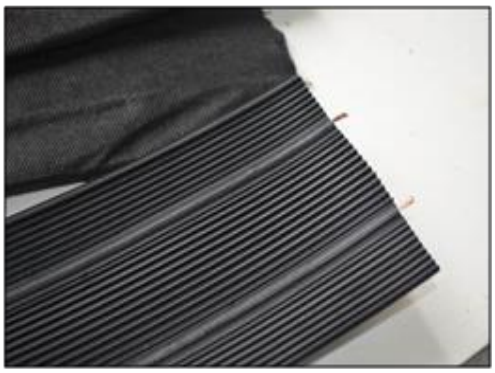

Figure 2. Photograph of the tabular EKG

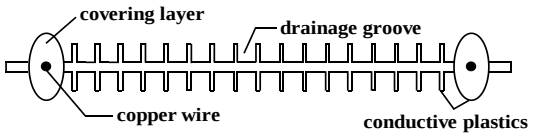

Figure 3. Schematic diagram of the tabular EKG

2.2 Experimental procedures

Five groups of laboratory tests were performed. The new tabular EKG was used as the electrode material, and five voltage gradients were employed. According to the preliminary test results, the test time for each test was set to 45 h. The basic parameters of the tests are summarized in Table 2.

Table 2. Basic parameters of the laboratory tests

Test numbers	Voltage gradients	Test time	Initial water content
T1	1.0 V/cm	45 h	61.58%
T2	1.5 V/cm	45 h	62.18%
T3	1.75 V/cm	45 h	61.73%
T4	2.0 V/cm	45 h	61.57%
T5	2.25 V/cm	45 h	62.05%

The specific test procedures were as follows. (1) A proper amount of dried soil was crushed. The

mass of water needed was calculated according to the assumption that the initial water content of the soil was 60%. The water was weighed following the calculation and poured into the soil. Then, the soil and water were thoroughly mixed using an electric mixer to create a remolded soil sample. The remolded soil was kept stationary for 24 h, after which its water content was measured. (2) After wrapping a geotextile around the outer surface of the tabular EKG, the EKG was placed at the corresponding position of the sample slot and served as both the cathode and the anode in the test. (3) The soil was emplaced in four layers to make it denser through packing. A cylinder was placed under the small hole of the collection tank. This cylinder was used to collect the water from the electro-osmotic process. (4) Voltage probes were inserted 37.5 mm, 75 mm, and 112.5 mm from the cathode and the vicinity of electrodes to measure the soil voltage. The inserted depth was 65 mm. (5) The wires, power supply and electrodes were connected. The power supply output voltage was adjusted to the voltage gradient set for the test. The circuit was connected. (6) Current readings were recorded every half-hour. Meanwhile, the soil voltages and liquid volumes were measured. (7) After 45 h, the test was stopped, and the power supply was disconnected. (8) The appropriate amount of the soil was selected near the vicinity of the electrodes. Some of the soil was freeze-dried to prepare experimental samples for scanning electron microscope (SEM). The other part was dried. Then, the soil was crushed by a mortar and sifted through a 0.075 mm sifter. The chemical composition of the soil was examined by X-ray fluorescence (XRF). (9) Finally, the test was completed, and the test devices were dismantled.

3. RESULTS AND DISCUSSION

After completing the electro-osmotic treatment, significant changes in the phenomenological characteristics of the soil samples and electrodes were observed (see Fig. 4). Most notably, the geotextile wrapped around the anode component of the EKG changed from white to yellow; in addition, the surrounding soil cracked, and the electrodes were separated from the upper soil. These macroscopic phenomena provided clues for the later data analysis.

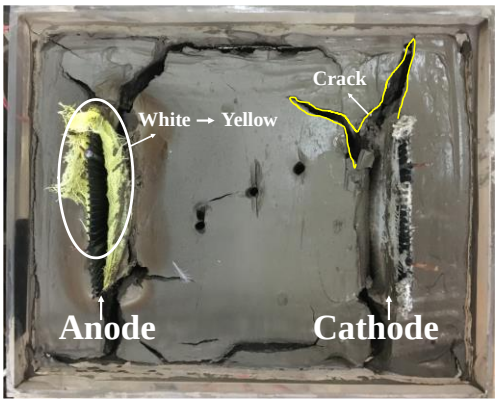

Figure 4. Changes in the phenomenological characteristics of the soil and electrodes at the end of electro-osmosis test

3.1 Macro level

The test results were compared and analyzed at the macro level by monitoring four, indexes,

namely, the volume of drained water, current, voltage and energy consumption. For each index, the variation in the electro-osmotic effect with the voltage gradient was explained, providing a basis for further comparison and analysis at the micro and theoretical levels.

3.1.1 Volume of drained water

The variations in the volume of drained water over time for all tests are illustrated in Fig. 5. A comparison of tests T1-T5 shows that both the drainage velocity and the drainage volume were high during the early stage of the electro-osmotic process at high voltage gradients, in accordance with previous studies [20]. However, the electro-osmotic drainage velocity at a high voltage gradient was lower than that at a low voltage gradient during the later stage of the experiment.

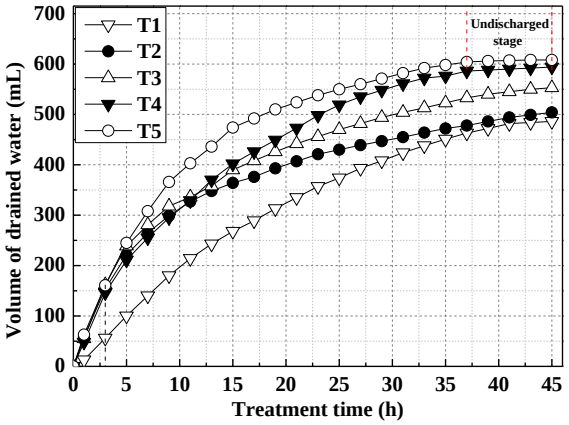

Figure 5. Volume of drained water variations over treatment time during the electro-osmotic process for various voltage gradients (T1=1 V/cm, T2=1.5 V/cm, T3=1.75 V/cm, T4= 2V/cm, T5=2.25 V/cm)

In addition, Fig. 5 shows that the variation tendency of the volume of drained water changed with an increase in the voltage gradient for all five tests. T1, T2 and T3 were divided into two main stages. The volume of drained water maintained a linear relationship with time in the first half of the test, during which the electro-osmotic drainage velocity remained nearly constant; however, the linear relationship gradually became curved in the second half of the test, and the drainage velocity decreased gradually. The same results were obtained by Kaniraj, Glendinning and Li [20-22]. Therefore, the relationship between the volume of drained water and time for tests T1-T3 showed a gradual change from a linear stage, in which the drainage velocity remained essentially unchanged, to a curved stage, in which the drainage velocity decreased gradually. Moreover, for the volume of drained water variation curves of T4-T5 in addition to those of the two abovementioned stages in T1-T3, a lack of discharge was observed for the electro-osmotic processes of T4 and T5; at the undischarged stage, the electro-osmotic drainage velocity was zero. This result demonstrated that the duration of electro-osmotic treatment decreased with an increase in the voltage gradient. Furthermore, a comparison of T2, T3, T4 and T5 shows that the volume of drained water was approximately the same during the first 3 h; at this stage, the electro-osmotic drainage effects among the four groups were equal, and the total energy consumption generated by the electro-osmotic process increased with the voltage gradient. Considering that the voltage gradients

increased in the order of T2 < T3 < T4 < T5, the extents of the total energy consumption increased in the same order. Thus, a relatively low voltage gradient could be used during the early stage of the test, while the gradient could be gradually increased during the later testing stage. Devices that use this approach are categorized as stepped voltage technologies; accordingly, some scholars have begun to conduct research on stepped voltage technology [23]. If this technology is used for electro-osmotic treatment, the total energy consumption of the electro-osmotic process can be effectively reduced while achieving a better electro-osmotic drainage effect.

3.1.2 Current

The current variations for all the laboratory tests are shown in Fig. 6. At the beginning of each test, the current increased with the voltage gradient. Overall, the variations in the current were consistent, that is, the current first increased and then decreased. This behavior is consistent with the results of Tuan [24]. The currents of T4 and T5 began to decrease at 0.5 h, whereas that of T3 decreased at 1 h, that T2 decreased at 1.5 h, and that of T1 decreased at 2 h. These phenomena were attributed to the redistribution of charge in the soil under the action of the electric field force at the start of the test. Initially, positive and negative charges were gathered in the cathode and anode, respectively, and the soil resistance became weakened during the charge accumulation process. Hence, the current showed a temporary rise; Zhuang explained this phenomenon in greater detail [25]. Shortly afterwards, the contact resistance between the electrodes and the soil increased with an increase in the electrification time, leading to a decrease in the current. Given that the voltage gradients of T4 and T5 were relatively large, the charge redistribution rate and the rate of increase in the contact resistance were higher than those of the other three groups. Consequently, the currents of T4 and T5 decreased before those of T1, T2 and T3. Similarly, the times at which the currents of the other three tests decreased rose following the sequence T3 < T2 < T1. Consequently, at the end of the test, the current of T1 was slightly higher than those of the other four groups. This result was obtained because the voltage gradient of T1 was the lowest; thus, the electro-osmotic drainage effect of T1 was relatively poor, and more water was retained in the soil.

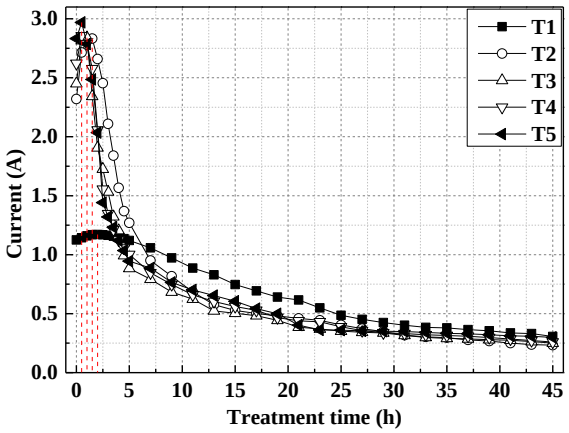

Figure 6. Current variations over treatment time during the electro-osmotic process for various voltage gradients (T1=1V/cm, T2=1.5V/cm, T3=1.75V/cm, T4=2V/cm, T5=2.25V/cm)

3.1.3 Voltage

Fig. 7 shows the voltage distributions of T1-T5 at different times. Overall, the voltage demonstrated an approximately linear distribution throughout the electro-osmotic process (see S1), except for an obvious change near the anode (see S2). Similar experimental results were reported by Jiao and Estabragh [26-27]. The straight slope near the anode increased with the electrification time. This phenomenon occurred mainly because the water near the anode was continuously discharged under electro-osmotic action. The result was a rapid increase in the soil resistance. However, the slope of S1 decreased gradually with an increasing electrification time, and the slope variation increased with the voltage gradient. These results show that the decay rate of the soil voltage increased with the voltage gradient.

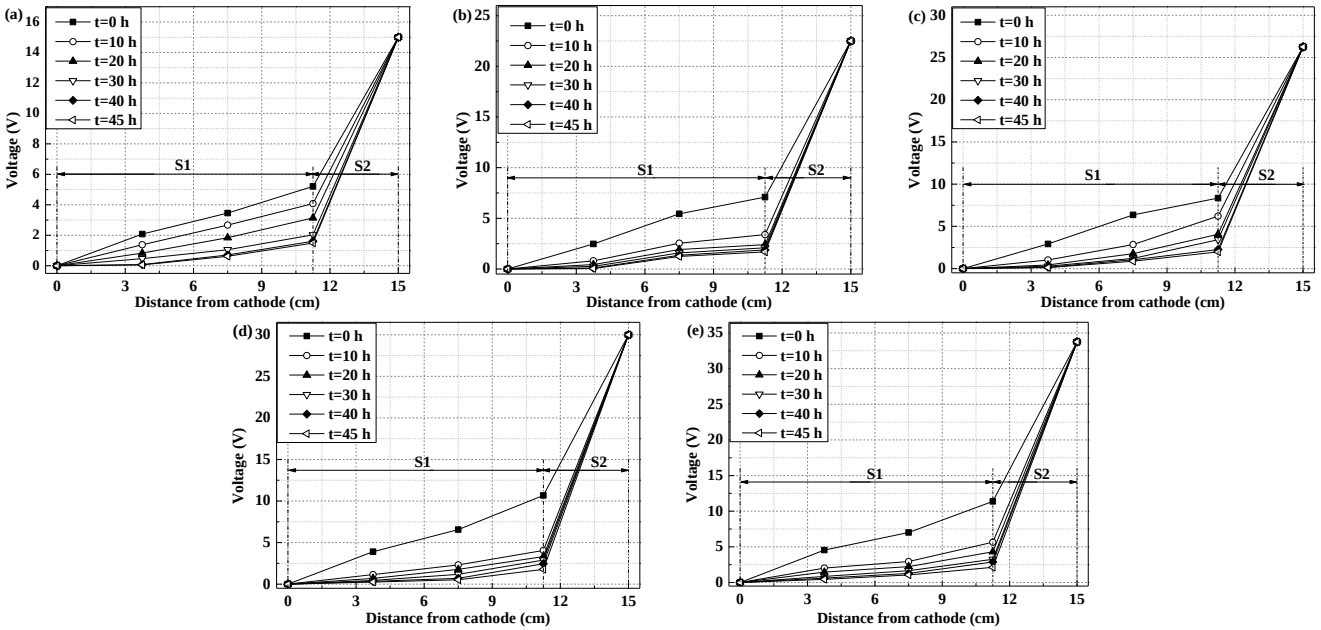

Figure 7. Voltage distributions at different times during the electro-osmotic process for various voltage gradients: (a) voltage distributions at different times under a voltage gradient of 1V/cm; (b) voltage distributions at different times under a voltage gradient of 1.5V/cm; (c) voltage distributions at different times under a voltage gradient of 1.75V/cm; (d) voltage distributions at different times under a voltage gradient of 2V/cm; (e) voltage distributions at different times under a voltage gradient of 2.25V/cm

Moreover, the output voltage of the power supply was consumed due to the interfacial resistance between the electrode and the soil. The voltage, which plays an effective role in the electro-osmotic consolidation of soil, can be equated to the voltage difference between the cathode and the anode, such as the voltage difference between V1 and V5 in Fig. 1. This voltage is called the effective voltage [28].

Fig. 8 shows the variations in the effective voltage over time. Overall, the effective voltage reached its maximum value at the onset of electrification, after which it decreased rapidly; this phenomenon was also noted by Zhou [29]. The higher the voltage gradient was, the faster the decay rate became.

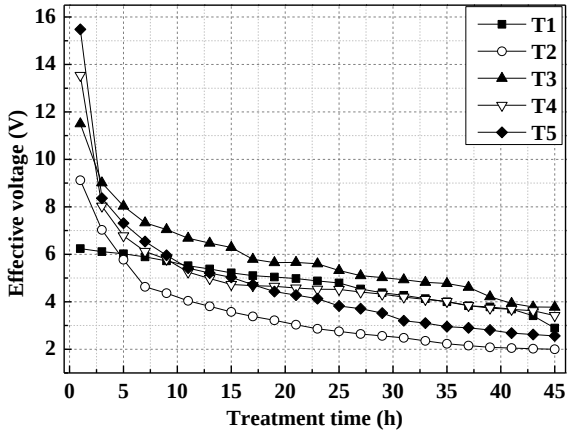

Figure 8. Effective voltage variations over treatment time during the electro-osmotic process for various voltage gradients (T1=1V/cm, T2=1.5V/cm, T3=1.75V/cm, T4=2V/cm, T5=2.25V/cm)

The onset of electrification represented a state of instantaneous excitation at which electro-osmotic flow had not yet been generated. Correspondingly, the decay rate of the effective voltage gradually became gentler with the continuous transformation of electrical energy into water flow, heat flow and electrochemical flow. In other words, the decay rate approached an approximately linear form. The higher the voltage gradient was, the larger the change in the decay rate of the effective voltage and the longer the time required for the decay rate to reach a constant value.

In addition, the ratios of the effective voltage of each of the five groups to the output voltage of the power supply were 19.27%~41.6%, 8.89%~43.64%, 14.36%~43.81%, 11.4%~45.13% and 7.59%~45.87%. These results indicate that an increase in the voltage gradient improved only the ratio of the effective voltage to the output voltage during the early stage of the electro-osmotic process. However, from a long-term perspective, increasing the voltage gradient was not useful for increasing the ratio of the effective voltage to the output voltage. This finding convincingly supports the results from the preceding analyses of the volume of drained water and current. Furthermore, compared with the other four groups, T1 showed a good linear relationship. This phenomenon occurred because the T1 voltage gradient was the lowest. The variations in the heat energy and electrochemical energy produced by the electro-osmotic process were not significant, and thus, the effective voltage did not rapidly decay.

3.1.4 Energy consumption per unit volume drainage

Its high energy consumption is one of the reasons why the electro-osmotic technique has not been popularized and applied at a broader scale [30]. Therefore, the electro-osmosis energy consumption must be taken into account when it is applied to treat soft clay foundations. The total energy consumption of the entire electro-osmotic process can be expressed as *W*.

$$W = \int_0^t UI\mathrm{d}t \tag{1}$$

The average energy consumption per unit volume drainage after the electro-osmotic process can be expressed as *C*.

$$C = \frac{W}{Q} \tag{2}$$

where U is the output voltage of the DC power supply, I is the current throughout the treatment, and Q is the drainage at the end of the electro-osmotic process. The current intensity is combined with the output voltage of the power supply in the electro-osmotic process, and thus, the energy consumption per unit volume drainage can be obtained according to Eqs. 1 and 2.

The results in Fig. 9 show that a high voltage gradient led to a high energy consumption per unit volume drainage, indicating that an excessive voltage gradient was not always better. The higher the voltage gradient was, the higher the drainage velocity became; however, the energy consumption per unit volume drainage also increased. Thus, a reasonable voltage gradient should be determined to achieve effective electro-osmotic treatment while effectively reducing its corresponding energy consumption. This optimal gradient should be determined according to the actual time and costs associated with a project when the electro-osmotic method is used to treat foundations composed of Taizhou soft clay.

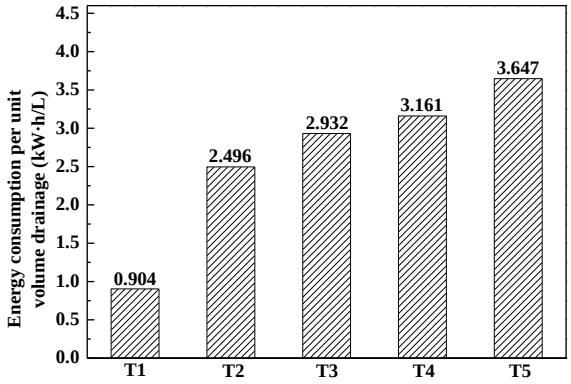

Figure 9. Energy consumption per unit volume drainage at the end of each test for various voltage gradients (T1=1V/cm, T2=1.5V/cm, T3=1.75V/cm, T4=2V/cm, T5=2.25V/cm)

3.2 Micro level

Many scholars have conducted numerous studies on the electro-osmotic process; however, most of those investigations provided descriptions and data analysis only at the macro level. As a result, insufficient research has been performed at the micro level, and thus, the microscopic mechanism of electro-osmosis is unclear at present. Consequently, to further explore the microscopic effects and mechanism of the electro-osmotic process under different voltage gradients, this study examined the migration of ions in soil under the action of an electric field and the change in the soil structure from before to after the electro-osmotic process. Then, reasonable explanations for the abovementioned macroscopic phenomena were provided from a microscopic perspective. The results of the micro-level analysis are as follows.

3.2.1 Element mass fraction of soil

The migration of ions can be reflected by the changes in the element mass concentrations. To study the ion migration patterns during the electro-osmosis process, the soil element mass fractions near the electrodes were analyzed after electro-osmosis treatment [10]. The mass fractions of two nonmetallic elements, i.e., Si and S, and the mass fractions of four metallic elements, i.e., Na^+, Al^{3+}, Ca^{2+}, and Mg^{2+}, were analyzed using XRF. The test results are shown in Fig. 10, in which A represents the anode, and C represents the cathode.

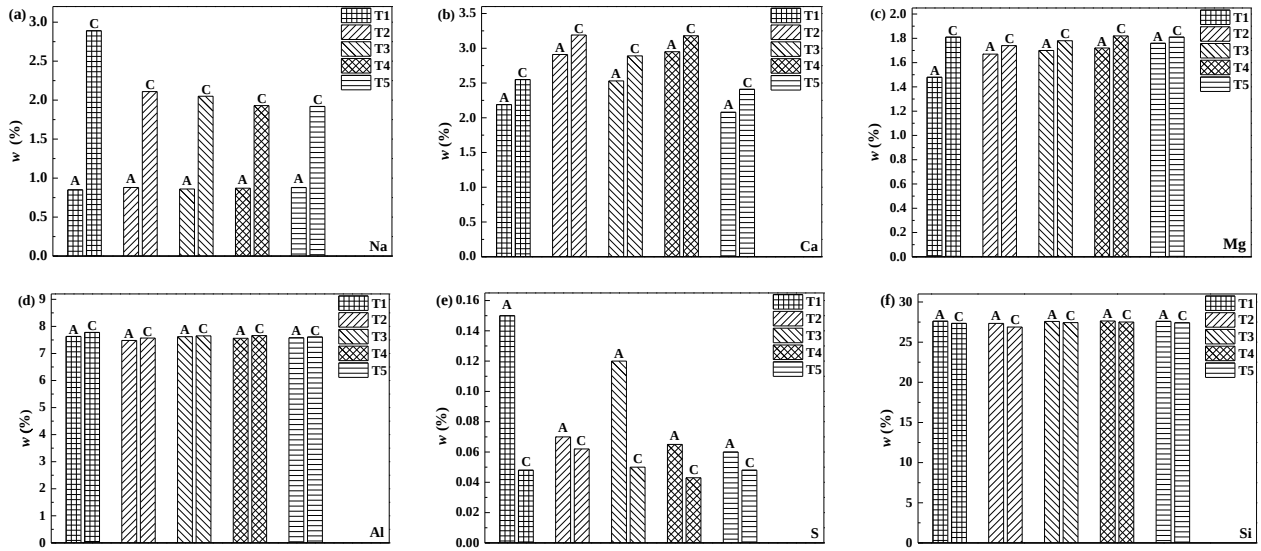

Figure 10. (a) Contents of sodium element in the soil mass at the anode and cathode electrodes after electro-osmosis process for various voltage gradients (T1=1 V/cm, T2=1.5 V/cm, T3=1.75 V/cm, T4= 2V/cm, T5=2.25 V/cm), (b) contents of calcium element, (c) contents of magnesium element, (d) contents of aluminum element, (e) contents of sulfur element, and (f) contents of silicon element

Overall, the contents of the nonmetallic elements at the anode were higher than those at the cathode, while the contents of the metallic elements were lower at the anode than those at the cathode. These results are in accordance with previously reported findings [29]. Thus, the metallic cations gradually migrated from the anode to the cathode under the action of the electric field, whereas the nonmetallic cations moved toward the anode. The quantity of migrated Na^+ was greater than those of the other three metallic elements. Na^+ constitutes the main ion in Taizhou soft clay and hence plays a leading role in the electro-osmotic drainage process with respect to the quantity of migrated Na^+ in the soil.

Compared with that of Na^+, the migrated quantities of the other three metallic elements were negligible. The quantity of migrated Al^{3+} was less significant than those of both Ca^{2+} and Mg^{2+}. Considering the migrated quantities of S and Si, the abovementioned phenomena were attributed to the migration of high-valence cations toward the cathode under the action of an electric field, whereas the anions of sulfate radicals and silicic acid in addition to other anions migrated toward the anode. These

cations and anions met in the middle area of the soil during their opposing migration, resulting in an electrochemical reaction that produced insoluble chemicals. Consequently, the cations did not reach the cathode successfully; similarly, the anions did not reach the anode successfully. In addition, Al^{3+} was more likely to participate in an electrochemical reaction because the activity of Al^{3+} was greater than those of Mg^{2+} and Ca^{2+} according to previous research results [31]. Ultimately, the quantity of migrated Al^{3+} was less evident than those of Ca^{2+} and Mg^{2+}. The rates at which these high-valence metallic cations contributed in the electro-osmotic process were low; thus, the cations failed to achieve their potential. This failure was one of the reasons that a higher-voltage gradient did not further improve the electro-osmotic drainage effect. In follow-up studies, more electrolyte solution can be added to the soil to ensure that additional high-valence metallic cations can become involved in the electro-osmotic process to further improve the electro-osmotic drainage effect.

Furthermore, Fig. 10 (a) shows that the Na^+ contents of T1-T4 at the anode were essentially the same, while the Na^+ contents at the cathode decreased in the order T4 < T3 < T2 < T1. These phenomena were attributed to the voltage gradient of T4 being higher than those of the other three groups; hence, the electro-osmotic drainage of T4 was the largest according to the drainage variation curve, and thus, a greater quantity of Na^+ moved toward the cathode and was discharged under the action of the electric field. Meanwhile, the Na^+ contents of T4 and T5 at the cathode were essentially the same at the ends of the tests. This consistency was observed because the contents of migrated Na^+ were limited in the electro-osmotic process, while the voltage gradients of T4 and T5 were relatively high. The electro-osmotic drainage velocity was very high during the early stage; correspondingly, almost all Na^+ was involved in the migration process during the early stage of the experiment, whereas little Na^+ migrated during the later stage, causing little water to be discharged. The later stage was thus considered the undischarged stage. These findings explain why the electro-osmotic drainage effect was not further improved by increasing the voltage gradient beyond 2 V/cm. As previously mentioned, Na^+ was the key factor that influenced the drainage effect and drainage velocity of the electro-osmotic process. The same conclusion has been drawn by other scholars despite the use of different test soils [31-33].

3.2.2 Soil structure

Considering that the electro-osmotic treatment effect achieved near the anode was the best, the soil near the anode was gathered and dried by freezing. Subsequently, the soil structure was studied using a QUANTA200 SEM. Fig. 11 shows the structure of Taizhou soft clay at the anode before and after electro-osmosis.

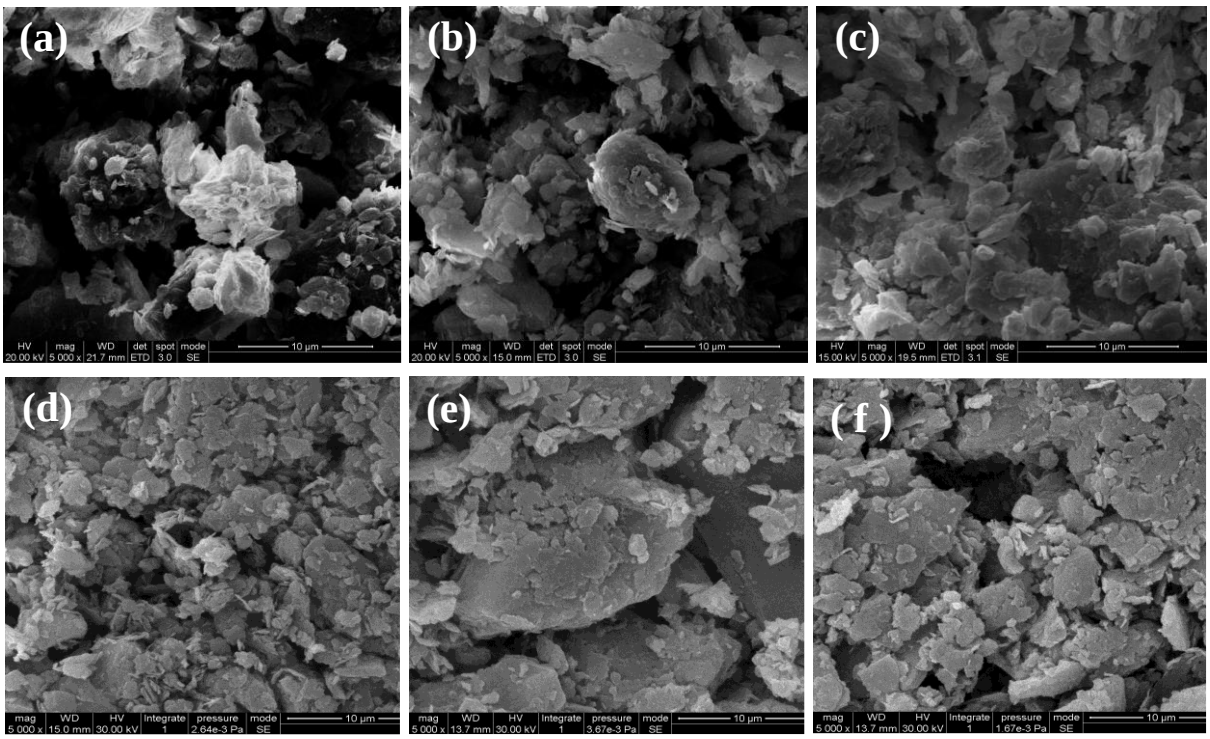

Figure 11. Scanning electron micrographs of the soil sample at the anode before and after electro-osmosis process (5000 times magnification): (a) the SEM image of soil sample before electro-osmosis, (b) the SEM image of soil sample at the end of T1 test (1 V/cm), (c) the SEM image of soil sample at the end of T2 test (1.5 V/cm), (d) the SEM image of soil sample at the end of T3 test (1.75 V/cm), (e) the SEM image of soil sample at the end of T4 test (2 V/cm), and (f) the SEM image of soil sample at the end of T5 test (2.25 V/cm)

Fig. 11 (a) shows an SEM image of the soil captured before electro-osmosis. The basic skeleton of the soft clay was composed of clay aggregates. The clay slices were wavy or crumpled. The particles were characterized mainly by face-to-face and face-to-edge contacts. The soft clay exhibited a flocculent appearance characterized by a loose structure and high porosity. This structure is one of the reasons why Taizhou soft clay exhibits its characteristically low strength, high compressibility and high flow denaturation. Fig. 11 (b)-(f) shows SEM images of the soil for T1-T5 after electro-osmosis. The soft clay structure changed from having a flocculent to a granular appearance after electro-osmotic treatments T1 and T2 according to Fig. 11 (b) and Fig. 11 (c). The trellis pores among the particles were also reduced, the particles were shaped like irregular polyhedra, and there was no distinct directional arrangement.

Fig. 11 (d)-(f) shows that the soil structure changed from having a flocculent to a schistose appearance after electro-osmotic treatments T3, T4 and T5. The porosity among the soil particles decreased significantly. Short chains were mainly formed by the accumulation of clay slices, enabling the connections among the particles, that is, the contacts among the soil particles became tighter. Hence, the clay slices adopted tight schistose shapes after the electro-osmosis treatments. The particles were characterized mainly by face-to-face contacts with close, overlapping and directional arrangements. Some differences in the structure of the soil after electro-osmosis occurred due to differences in the voltage gradients applied. The soil structure changed from having a flocculent to a granular appearance

after electro-osmotic treatment when the voltage gradient was within the range of 1 V/cm~1.5 V/cm. In contrast, the soil structure changed from having a flocculent to a schistose appearance after electro-osmotic treatment when the voltage gradient was within the range of 1.75 V/cm~2.25 V/cm. Wu also found that the soil structure changes before and after electro-osmosis; however, their reported test results differed from those in this paper due to the use of different soil samples [33].

3.2.3 Porosity

SEM images of soil samples indicate both that changes in the soil structure can be qualitatively analyzed and that information regarding the pore arrangement, particle size and particle shape can be obtained [34]. First, the SEM images of the soil samples were processed. Then, the processed images were quantitatively analyzed using the 3D visualization and 3D analysis module provided in GIS. Accordingly, the 3D surface of the soil structure was reconstructed. Finally, the void ratio and porosity of the soil were calculated using an image analysis technique. Fig. 12 shows 3D visualizations of the soil samples.

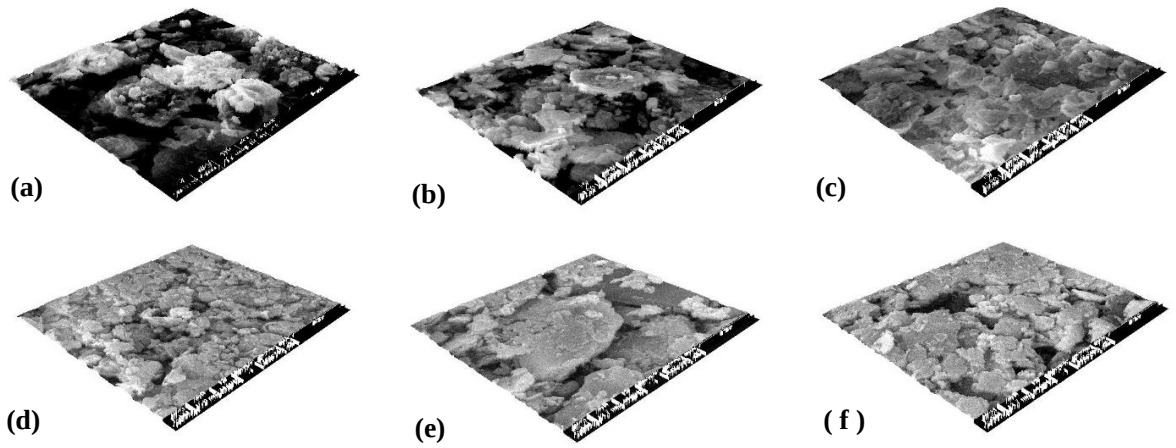

Figure 12. 3D visualizations of the soil surfaces before and after electro-osmosis process: (a) 3D visualization of the soil before electro-osmosis, (b) 3D visualization of the soil at the end of T1 test (1 V/cm), (c) 3D visualization of the soil at the end of T2 test (1.5 V/cm), (d) 3D visualization of the soil at the end of T3 test (1.75 V/cm), (e) 3D visualization of the soil at the end of T4 test (2 V/cm), and (f) 3D visualization of the soil at the end of T5 test (2.25 V/cm)

The void ratio and porosity of each soil sample were obtained using image analysis software, the results of which are shown in Table 3. The void ratio was 1.705 and the porosity of the soil was 63.03% before electro-osmosis process; after electro-osmosis treatment, the void ratio and porosities of the soil samples were reduced to varying degrees with different voltage gradients. The void ratio and soil porosity decreased significantly with an increase in the voltage gradient when the voltage gradient was within the range of 1.0 V/cm~1.75 V/cm. However, further decreases in the void ratio and soil porosity with an increase in the voltage gradient beyond 1.75 V/cm were not significant.

Table 3. Variations in the void ratio and porosity before and after electro-osmosis treatment

Tests numbers	Void ratio	Porosity
Untreated soil	1.705	63.03%
T1	1.057	51.39%
T2	0.576	36.54%
T3	0.202	16.84%
T4	0.200	16.69%
T5	0.177	15.03%

3.2.4 Fractal dimension values

The fractal dimension value is used to quantitatively describe the pores and structural characteristics of soil [35]. It is well known that a number of particles are included in an image ($L \times L$), and an image can be segmented into an orthogonal grid ($L/a \times L/a$) of squares ($a \times a$). The lattice number of grids containing soil particles is denoted as $N(a)$. The value of a is varied from small to large, for example, $a1$, $a2$, and $a3$; consequently, $N(a1)$, $N(a2)$ and $N(a3)$ are obtained. These data are expressed in dual logarithmic coordinates, as the expressions $\ln(a)$ and $\ln N(a)$ share distinct linear characteristics. Their relationship can be used to represent the fractal characteristics of soil particles. If the slope of the linear part is K, the fractal dimension value of the soil particles can be expressed as D_p.

$$D_p = -\lim_{a \to 0} \frac{\ln N(a)}{\ln(a)} = -K \tag{3}$$

Studies have shown that a larger fractal dimension value corresponds to a more dispersed soil particle distribution, a lower degree of grouping and a denser collection of soil particles. Based on the abovementioned algorithm, the SEM images were first binarized. Then, the processed images were divided into many orthogonal grids with different side lengths. The total number of related grids was used to draw the scatter diagram of $\ln N$(a) versus $\ln(a)$. Then, the results were fitted, as shown in Fig. 13.

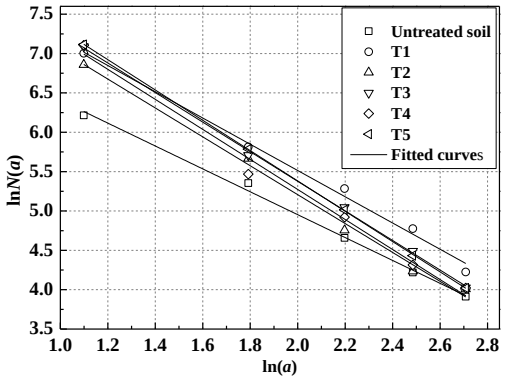

Figure 13. Fractal dimension values of the soil samples before and after electro-osmosis treatment for various voltage gradients (T1=1 V/cm, T2=1.5 V/cm, T3=1.75 V/cm, T4=2 V/cm, T5=2.25 V/cm)

The fractal dimension value of the soil was 1.454 before electro-osmotic treatment. After electro-osmotic treatment, the corresponding values for T1, T2, T3, T4 and T5 were 1.668, 1.836, 1.879, 1.908 and 1.926, respectively. The fractal dimension values of the soil particles clearly increased from T1 to T5 after electro-osmotic treatment. This finding indicates that the soil became denser after electro-osmotic treatment. However, a further increase in the fractal dimension value with an increase in the voltage gradient beyond 1.5 V/cm was not evident.

In summary, the macro-level analysis showed that the electro-osmotic drainage effects differed under the five voltage gradients, and those differences can be reasonably explained based on the variations in the current and voltage during the electro-osmotic process. At the micro level, the mass contents of the major elements in the soil and the soil structure were measured. The results indicated that Na^+ was the main active ion within Taizhou soft clay during the electro-osmotic process; furthermore, the migratory content of Na^+ was the key factor that affected both the drainage and the drainage velocity of the electro-osmotic treatment. Other high-valence cations contributed less to the electro-osmotic process due to electrochemical problems. When the voltage gradient was within the range of 1 V/cm~2 V/cm, an increase in the voltage gradient increased the migration content of Na^+ such that additional water could be discharged. However, the content of migrated Na^+ was limited throughout the electro-osmotic process, and the drainage velocity of the electro-osmotic process was very high when the voltage gradient was within the range of 2 V/cm~2.25 V/cm. Nearly all Na^+ was involved in the migration process during the early stage of the experiment, and thus, little Na^+ was involved in the migration during the later stage. Accordingly, the electro-osmotic effect was not significant during the later stage of the experiment, and little water was discharged therein.

Furthermore, some differences were observed in the soil structure under the different voltage gradients after electro-osmotic treatment. When the voltage gradient was within the range of 1 V/cm~1.5 V/cm, the structure of the soil changed from exhibiting a flocculent to a granular appearance. When the voltage gradients were within the range of 1.75 V/cm~2.25 V/cm, the soil structure changed from having a flocculent to a schistose appearance after electro-osmotic treatment. The abovementioned results show that differences in the content of migratory Na^+ and changes in the soil structure resulted in variations in either the current or the voltage during the electro-osmotic process. In turn, these variations led to differences in the electro-osmotic drainage effect under different voltage gradients.

3.3 Theoretical level

As discussed in the previous section, laboratory model tests of EKG electro-osmosis were conducted under different voltage gradients, and the experimental results were analyzed at both the macro level and the micro level. The porosity of the soil was reduced to varying degrees after the electro-osmotic treatment according to an analysis of the soil porosity variations at the micro level, indicating that the soil became consolidated during the electro-osmotic process. In addition, the contact area between the EKG electrode and the soil was changed due to the reduction in the soil volume; this alteration had a certain influence on the soil voltage. Furthermore, combined with an analysis of the soil voltage distribution at the macro level, the soil voltage clearly decreased with the implementation of the electro-osmotic treatment. The findings are different from those suggested by the current electro-osmotic

consolidation theory, in which the soil voltage is assumed to remain constant at each point [36-38].

The effective voltage of the soil was lower than the output voltage of the power supply due to the contact resistance between the soil and the electrodes during the electro-osmotic process. Therefore, the electro-osmotic treatment effect could be overestimated if the influences of variations in the soil voltage are not considered in the deduction of electro-osmotic theory; of course, such an overestimation would be highly unfavorable for engineering construction [39]. In the current study, a new one-dimensional electro-osmotic consolidation equation was established to more reasonably reflect the consolidation of soil during the electro-osmotic process. The equation was based on the above analyses conducted at the macro and micro levels, and the variation trend of the effective voltage was explored. Ultimately, a new analytical expression for the excess pore water pressure was deduced. The resulting expressions are intended to provide a reference for the subsequent promotion and application of the electro-osmotic method.

3.3.1 Basic assumptions

The following basic assumptions were made to establish a new one-dimensional electro-osmotic consolidation equation considering variations in the effective voltage.

(1) The soil is fully saturated and homogeneous. Decreases in the number of soil particles and the pore water content during consolidation can be neglected. (2) The drainage amount discharged from a unit cell of soil is equal to the decrease in the soil volume. (3) The coefficients of the hydraulic permeability and electric permeability of the soil are assumed to be constant during consolidation. (4) The movement of water flow caused by various chemical concentrations and heat is not considered. (5) Compressive strains are allowed to occur only in the vertical direction. (6) The flow caused by the electrical gradient can be superimposed with the flow caused by the hydraulic gradient.

3.3.2 Establishing an effective voltage expression

The parameters at the macro and micro levels were studied to enable the one-dimensional electro-osmotic consolidation equation to more universally consider variations in the effective voltage. An inherent link among the parameters was found, and the rules governing the effective voltage variation were determined, thereby enabling the new consolidation equation considering variations in the effective voltage to better serve engineers in practice.

Voltage gradients and fractal dimension values

Upon fitting the data, the applied voltage gradients and the calculated fractal dimension values displayed an approximately linear relationship. The fitting results are shown in Fig. 14. The degree of anastomosis is 97.61%, and the relationship between the two sets of results can be written as follows.

$$Y = 0.2227X + 1.463 \tag{4}$$

where Y is the fractal dimension value and X is the voltage gradient. Thus, the fractal dimension value can be determined once the voltage gradient is determined.

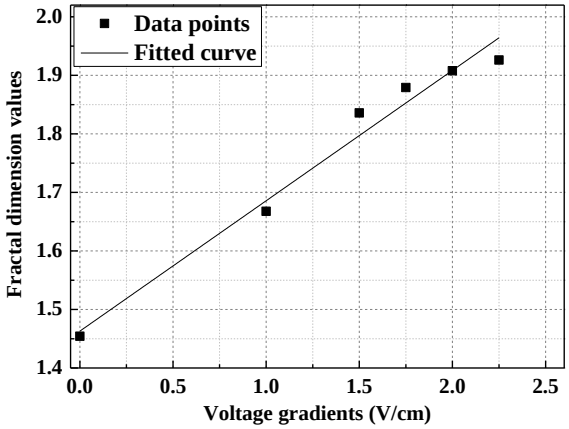

Figure 14. Fractal dimension values variations over the voltage gradients at the end of each test

Effective voltage

A logarithmic relationship was observed in which the effective voltage decreased over time. Thus, the effective voltage was fit logarithmically, and the fitting results are shown in Fig. 15.

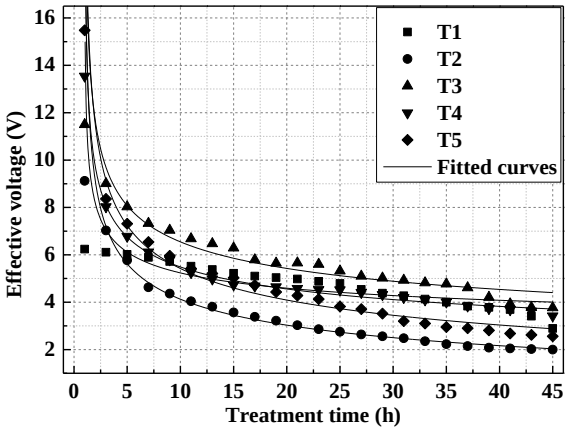

Figure 15. Fitted curves of the effective voltage with treatment time for various voltage gradients (T1=1 V/cm, T2=1.5 V/cm, T3=1.75 V/cm, T4=2 V/cm, T5=2.25 V/cm)

The relationships between the time and effective voltage among the five groups are written as follows.

$$\mathrm{T1}: \varphi_1(L,t) = -0.870\ln(t) + 7.2552 \quad (5)$$

$$\mathrm{T2}: \varphi_2(L,t) = -1.842\ln(t) + 8.7229 \quad (6)$$

$$\mathrm{T3}: \varphi_3(L,t) = -1.897\ln(t) + 11.277 \quad (7)$$

$$\mathrm{T4}: \varphi_4(L,t) = -2.102\ln(t) + 11.088 \quad (8)$$

$$\mathrm{T5}: \varphi_5(L,t) = -2.838\ln(t) + 12.884 \quad (9)$$

where L is the distance between the cathode and the anode and t represents time. The effective voltage at any voltage gradient can be written as follows.

$$\varphi(L,t) = M\ln(t) + N \tag{10}$$

where M and N are coefficients related to the voltage gradient.

Fractal dimension values and the corresponding coefficients (*M, N*)

Upon fitting the data, the fractal dimension values and the corresponding coefficients (M, N) displayed approximately linear relationships. The fitting curves are shown in Fig. 16. The fitting accuracy of M is 93.3%, and that of N is 95.6%. The corresponding expressions are written as follows.

$$M = -5.2601Y + 7.7635 \tag{11}$$

$$N = 24.628Y\text{-}35.269 \tag{12}$$

If Eq. 4 is combined with Eqs. 11 and 12, the relationships between the coefficients and the applied voltage gradient can be written as follows.

$$M = -1.17X + 0.068 \tag{13}$$

$$N = 5.485X + 0.402 \tag{14}$$

The coefficients (M, N) can be determined for the corresponding voltage gradient once the voltage gradient is determined.

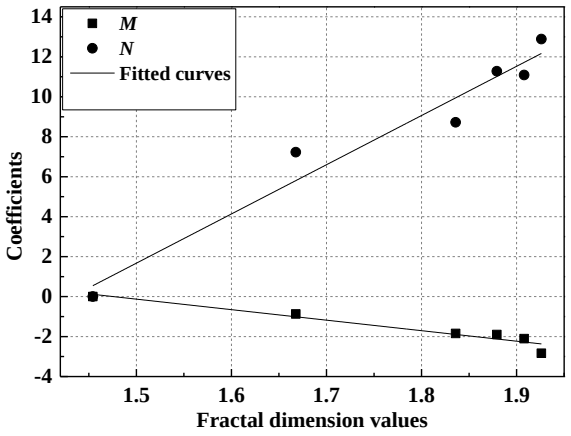

Figure 16. Variations in the coefficients (M, N) with the fractal dimension values

3.3.3 Deduction of the consolidation equation

The electro-osmotic pore water flow velocity is coupled with the hydraulic gradient flow and electrical gradient flow according to assumption (6).

$$q_h = k_h i_h + k_e i_e \tag{15}$$

The following expressions can be obtained if assumptions (1) and (2) are combined with Terzaghi's one-dimensional consolidation theory.

$$divq_h = m_v \frac{\partial u}{\partial t} \tag{16}$$

$$divq_h = \frac{\partial q_h}{\partial x} = \frac{k_h}{\gamma_w}\frac{\partial^2 u}{\partial x^2} + k_e \frac{\partial^2 \varphi}{\partial x^2} = m_v \frac{\partial u}{\partial t} \tag{17}$$

where u is the excess pore water pressure, φ is the voltage, k_h and k_e are the coefficients of the hydraulic

permeability and electro-osmotic permeability, respectively, x is the distance from the cathode, γ_w is the density of water, t is time, m_v is the soil volume compressibility coefficient and q_h is the electro-osmotic pore water flow velocity. Moreover, the effective voltage at any distance from the cathode under any voltage gradient can be written as follows according to Eq. 10.

$$\varphi(x,t) = (MIn(t) + N)\frac{x}{L} \tag{18}$$

The variable ξ is introduced such that $\xi(x,t) = u(x,t) + \frac{k_e\gamma_w}{k_h}\varphi(x,t)$. The following expressions can be obtained if Eqs. 17 and 18 are combined.

$$\frac{\partial\xi}{\partial t} = c_h\frac{\partial^2\xi}{\partial x^2} + f(x,t) \tag{19}$$

$$f(x,t) = \frac{k_e\gamma_w}{k_h} \times \frac{Mx}{tL} \tag{20}$$

Eq. 19 is the one-dimensional electro-osmotic consolidation equation considering variations in the effective voltage. In addition, the anode is closed, and the cathode is open; thus, the boundary conditions are expressed as follows.

$$\xi(0,\ t) = 0 \tag{21}$$

$$\xi_x(L,\ t) = 0 \tag{22}$$

The initial conditions are as follows.

$$\xi(x,0) = u(x,0) + \frac{k_e\gamma_w}{k_h}\varphi(x,0) \tag{23}$$

The expression for the excess pore water pressure is obtained by separation of variables.

$$u(x,t) = -\frac{k_e\gamma_w}{k_h}\varphi(x,t) + u_1(x,t) + u_2(x,t) \tag{24}$$

$$u_1(x,\ t) = \sum_{k=0}^{\infty}\frac{8k_e\gamma_w\varphi_0(-1)^k}{k_h(2k+1)^2\pi^2} \times \exp(-(k+\frac{1}{2})^2\pi^2T_v) \times \sin((k+\frac{1}{2}) \times \frac{\pi}{L}x) \tag{25}$$

$$u_2(x,t) = \sum_{k=0}^{\infty}\int_0^t \frac{\exp((k+\frac{1}{2})^2\frac{\pi^2c_h}{L^2}\tau)}{\tau}d\tau \times \frac{8k_e\gamma_w(-1)^kM}{k_h(2k+1)^2\pi^2} \tag{26}$$

$$\times \sin((k+\frac{1}{2}) \times \frac{\pi}{L}x) \times \exp(-(k+\frac{1}{2})^2\pi^2T_v)$$

$$Tv = \frac{c_ht}{L^2} \tag{27}$$

The soil voltage is a constant value if M and N are both zero. Thus, Eq. 24 can be rewritten as follows.

$$u'(x,t) = -\frac{k_e\gamma_w}{k_h}\varphi(x,t) + u_1(x,t) \tag{28}$$

This result is consistent with the expression of the excess pore water pressure in Esrig's one-dimensional electro-osmotic consolidation theory.

3.4 Analysis of the sample

A test with a voltage gradient of 0.5 V/cm was conducted to verify the rationality of the one-dimensional electro-osmotic consolidation equation considering variations in the effective voltage. The test materials, devices and procedures were essentially the same as those described above. The only difference was that two micro pore water pressure gauges were embedded near the anode at a depth of 65 mm. Disturbances of the pore pressure gauges by the seepage field were neglected due to the small size of the pore pressure gauges. The pore pressure gauges were linked to the readout instrument through electric wires to record data.

By combining Eqs. 13 and 14 according to the magnitude of the applied voltage gradient, the correlation coefficients were determined to be M =-0.517 and N=3.142. Furthermore, the following basic soil parameters were obtained through preliminary tests. The electro-osmosis permeability (k_e) is 5×10^{-9} $m^2/s\bullet V$, the hydraulic permeability (k_h) is 2×10^{-8} m/s, the horizontal consolidation parameter (c_h) is 8×10^{-8} m^2/s, and L is 0.15 m. Then, these parameters were substituted into Eqs. 24 and 28. Using Esrig's theory, the theoretical value of the excess pore water pressure considering variations in the effective voltage could thus be obtained. Fig. 17 shows the calculated value of the excess pore water pressure considering variations in the effective voltage (value 1), the calculated value using Esrig's theory (value 2) and the dissipated value of the excess pore water pressure measured experimentally (value 3).

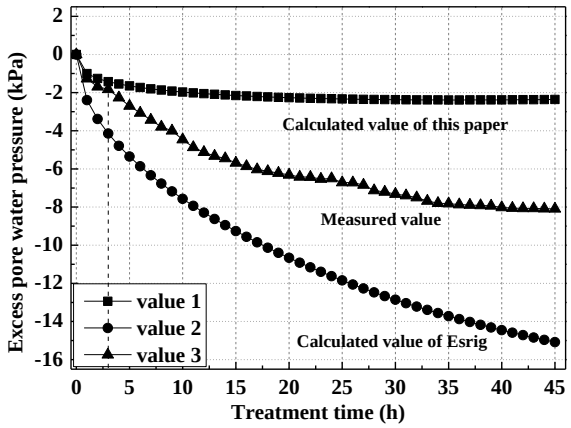

Figure 17. Comparison between the calculated and measured excess pore water pressure values under a voltage gradient of 0.5 V/cm

Clearly, value 2 was far greater than value 3; this occurred because the theoretical derivation did not take into account the real soil voltage. In fact, the effective voltage was much smaller than the external output voltage. Thus, the calculated value (value 2) was larger. Moreover, the dissipation trends of values 1 and 3 were consistent. Compared with value 2, value 1 was closer to the measured value. These results prove the reasonability of the one-dimensional electro-osmotic consolidation equation established in this study. In addition, the calculated value (value 1) agreed well with the measured value (value 3) during the first 3 h. However, the values varied 3 h later, following which the measured result was greater than the calculated result. This discrepancy was caused mainly by the following reasons. On the one hand, the probes that were used to measure the effective voltage were buried near the cathode

and anode; hence, the actual electrodes and probes were separated by a miniscule distance. Thus, the voltage measured using the probes was slightly lower than the actual effective voltage. In subsequent studies, the test error caused by this situation should be reduced. On the other hand, electrolytic exothermic effects and electrochemical reactions among the ions generated changes in the excess pore water pressure, whereas the analytical derivation neglected these actions; thus, the analytical value (value 1) was smaller than the measured value (value 3). These effects increased with the test duration; thus, value 3 ultimately diverged from value 1.

4. CONCLUSIONS

A series of one-dimensional electro-osmotic tests on Taizhou soft clay were performed under five different voltage gradients. The experimental results were analyzed from macro-level, micro-level and theoretical perspectives. The following conclusions can be drawn.

(1) The electro-osmotic drainage was effectively improved with an increase in the voltage gradient when the voltage gradient was within the range of 1 V/cm~2 V/cm. However, the drainage effect did not improve further by continuing to increase the voltage gradient. Furthermore, the duration of the electro-osmotic process decreased with an increase in the voltage gradient. Although an excessively high voltage gradient increased the drainage effect, such a high gradient led to a higher energy consumption per unit volume of drainage. Thus, the voltage gradient should be reasonably determined according to the construction period and cost before the electro-osmotic method is implemented.

(2) An increase in the voltage gradient improved only the ratio of the effective voltage to the output voltage in the early stage of the electro-osmotic process. However, from a long-term perspective, the increase in the voltage gradient was not useful for increasing the ratio of the effective voltage to the output voltage.

(3) Na^+ was the main active ion in Taizhou soft clay and played a leading role in the electro-osmotic process; moreover, Na^+ was the key factor that affected both the drainage and the drainage velocity of the electro-osmotic process. When the voltage gradient was within the range of 1 V/cm~2 V/cm, the content of migrated Na^+ increased with a rise in the voltage gradient during the electro-osmotic process. However, there was no significant improvement in the migration of Na^+ when the voltage gradient was increased further. Other high-valence cations contributed less to the electro-osmotic process due to electrochemical reactions.

(4) Taizhou soft clay exhibits a flocculent structure. Some differences were observed in the soil structure after electro-osmotic treatment due to the application of different voltage gradients. The soil structure changed from exhibiting a flocculent to a granular appearance after electro-osmotic treatment when the voltage gradient was within the range of 1 V/cm~1.5 V/cm. Moreover, the soil structure changed from having a flocculent to a schistose appearance after electro-osmotic treatment when the voltage gradient was within the range of 1.75 V/cm~2.25 V/cm. In addition, a larger voltage gradient corresponded to a smaller porosity and a larger fractal dimension value after electro-osmotic treatment. However, the rates of change of the porosity and fractal dimension values decreased gradually with an increase in the voltage gradient.

(5) Based on the inherent link between the macro and micro levels, a new one-dimensional electro-osmotic consolidation equation considering variations in the effective voltage was deduced. Compared with Esrig's equation, the new equation is more consistent with measured data. Additionally, the proposed equation can accurately forecast and assess changes in the excess pore water pressure during electro-osmotic treatment. The new equation is intended to serve as a reference for the subsequent application of electro-osmotic methods in the treatment of soft clay and the popularization of electro-osmotic methods in the future.

ACKNOWLEDGMENTS
This work was supported by the 111 Project of Ministry of Education of the People's Republic of China under Grant B13024.

References

1. T. B. Dennes, S. Inthuorn and H. Suksun, *Geotech. Test. J.*, 26(2003)277.
2. Y. M. Liu, X. X. Xie and L. W. Zheng, *Int. J. Electrochem.Sci*., 13(2018)9051.
3. Z. J. Xue, X. W. Tang and Q. Yang, *Dry. Technol*., 33(2015)986.
4. Y. Shen, H. D. Xu and W. J. Huang, *J. Civ. Eng. Manage*., 31(2014)7.
5. S. Micic and J. Q. Shang, *Can. Geotech. J*., 38(2001)287.
6. G. Lefebvre and F. Burnotte, 2002, *Can. Geotech. J*., 39(2002)399.
7. X. Q. Wang and W. L. Zou, *J. Wuhan Univ. Technol*., 24(2002)62.
8. Y. C. Hu, Z. Wang and Y. F. Zhuang, *Chin. J. Geotech. Eng*., 27(2005)582.
9. W. M. Kan, Y. H. Cao, *China Harbour Eng*., 28(2008) 71.
10. Y. L. Tao, J. Zhou and X. N. Gong, *J. Zhejiang Univ*. (*Eng. Sci*.)., 48(2014)1618.
11. A. Rittirong, J. Q. Shang and E. Mohamedelhassan, *J. Geotech. Geoenviron. Eng*., 134(2008)352.
12. Y. F. Zhuang and Z. Wang, *Rock Soil Mech*., 25(2004)117.
13. Y. H. Cao, J. F. Hou and Z. Y. Gao, *Geotech. Eng. Tech*., 24(2010)291.
14. L. J. Wang, S. H. Liu and Z. J. Wang, *Eng. Mech*., 30(2013)91.
15. Y. Wan and Q. Yang, *J. Water Resour. Archit. Eng*., 12(2014)94.
16. H. Wu, L. M. Hu and Q. B. Wen, *Appl. Clay Sci*., 111(2015)76.
17. Y. Li and X. N. Gong, *Chin. J. Rock. Mech. Eng*., 28(2009)4034.
18. P. Asavadorndeja and U. Glawe, *Bull. Eng. Geol. Environ*., 64(2005)237.
19. W. L. Zou, J. X. Yang and Z. Wang, *Chin. J. Geotech. Eng*., 24(2002)319.
20. S. R. Kaniraj, H. L. Huong and J. H. S. Yee, *Geotech. Geol. Eng*., 29(2011)277.
21. S. Glendinning, *J. Hazard. Mater*., 39(2007)491.
22. Y. W. Li, J. Zhou and X. N. Gong, *Rock Soil Mech*., 34(2013)1972.
23. F.Y. Liu, W. Mi and H. T. Fu, *Chinese J. Rock Mech. Eng*., 33(2014)2582.
24. P. Tuan, M. Sillanpää, *J. Hazard. Mater*., 173(2010)54.
25. Y. F. Zhuang, Z. Wang, *Rock Soil Mech*., 26(2005)629.
26. D. Jiao, X. N. Gong and Y. Li, Chinese J. Rock Mech. Eng., 30(2011)3208.
27. A. R. Estabragh, M. Naseha, and A. A. Javadi, *Appl. Clay Sci*., 95(2014)32.
28. L. W. Zheng, Y. X. Xie and K. H. Xie, *J. Southeast Univ*., 48(2018)557.
29. J. Zhou, Y. L. Tao, *Soils Found*., 55(2015)1171.
30. J. Wang, L. Zhang and F.Y. Liu, *Chin. J. Rock Mech. Eng*., 33(2014)4181.
31. K. S. Guo, Y. F. Zhuang and W. Duan, *J. Zhejiang Univ*., 51(2017)2373.
32. J. Peng, G. Q. Xie and B. Su, *J. Hohai Univ*., 44(2016)135.
33. H. Wu, L. M. Hu and G. P. Zhang, *J. Mater. Civ. Eng*., 28(2016)1.

34. B. J. Wang, B. Shi and Y. Cai, *Rock Soil Mech*., 29(2008) 251.
35. H. H. Mo, J. Wang and Y. X. Lin, *Chin. J. Rock Mech. Eng*., 32(2013)2465.
36. M. I. Esrig, J. P. Gemeinhardt, *J. Soil Mech. Found. Div*., 93(1967)109.
37. J. Q. Su, Z. Wang, *Rock Soil Mech*., 25(2004)125.
38. Y. LI, X. N. Gong and M. M. Lu, *Chinese J. Geotech. Eng*., 32(2010)77.
39. H. Wu, L. M. Hu, *Chin. J. Geotech. Eng.*, 35(2013)734.